Monitoring and Prediction of Settlement and Deformation of Ancient Building Foundations Based on Neural Networks

Lei Gao*, Heng Wang
School of Civil Engineering, Nanyang Normal University, Nanyang 474100, China
E-mail: yshanmo@163.com
*Corresponding author

Keywords: grey artificial neural network, settlement of ancient building foundations, deformation monitoring and prediction, deep beliefs, stress analysis

Received: April 11, 2024

With the rapid development of the tourism industry, the visual value of ancient buildings gradually increases. The prediction and protection of ancient building foundation settlement based on neural networks have been developed. When traditional methods are used to monitor and predict the settlement and deformation of ancient building foundations, complex factors such as water environment and geological conditions can bring noise to the experimental results. Deep belief was introduced into grey artificial neural networks to effectively denoise the corresponding model and enhance its ability to process data. Meanwhile, stress analysis was conducted on the ancient building foundation in the experiment to generate a composite model. Experiments were conducted on the Abfound dataset. Three models were compared to verify the predictive ability for ancient buildings, including random forest, to verify the superiority of the model. The dimensionality reduction capabilities of four models for building data were 4.6, 3.6, 3.2, and 3.9, respectively, indicating that the optimized model could effectively handle a large amount of data. The composite model had the highest accuracy in predicting the settlement of ancient building foundations, with an experimental data of 99.2%. These experiments confirmed that the proposed composite algorithm performed best in terms of noise reduction and prediction ability. This algorithm is suitable for predicting the settlement deformation of ancient building foundations.

Povzetek: Raziskava uvaja inovativni model za napovedovanje posedanja in deformacij temeljev starih zgradb, ki temelji na nevronskem omrežju z uporabo globokega prepričanja (deep beliefs) za zmanjševanje šuma. Eksperimenti na Abfound podatkovnem naboru so pokazali, da ima sestavljeni model najvišjo točnost pri napovedovanju posedanja temeljev.

1 Introduction

As the improvement of the national economy, residents' entertainment gradually focuses on urban buildings, and their protection requirements gradually increase [1-2]. Ancient buildings are an important component of cultural heritage, carrying memories of history and culture and possessing significant scientific value. The settlement and deformation of the foundation are the main problems they face [3]. The foundation often experiences settlement and deformation, due to the long history of urban construction and environmental changes, posing a serious threat to the safety and integrity of urban construction [4]. Many experts have proposed using neural networks to accurately predict them. However, these methods are only applicable to arbitrary building in limited terrain and humidity environments. The data accuracy of traditional neural networks is insufficient due to the complex natural factors. Recently, Grey Artistic Neural Network (GANN) has received attention due to its extensive search domain. However, the ordinary GANN has weak resolution ability and is prone to falling into local optima during operation. To address these issues, this study concatenated GANN to generate Series Grey Artistic Neural Network (SGANN) and introduced Deep Belief (DB) to generate a fusion model (DB-SGANN). A composite model (SPDB-SGANN) was generated by considering the Stability of Pile (SP) of arbitrary building. SPDB-SGANN improved the traditional grey prediction model and improved this model's stability by introducing nonlinear fitting ability. In this study, the improved GANN was applied to the monitoring and prediction of foundation settlement of ancient buildings to avoid problems such as building inclination and cracks. The main content of this study includes four parts. Firstly, the current applications of GANN are summarized. Secondly, the usage of SP is introduced and introduced into DB-SGANN. The third part conducts simulation experiments. Finally, the model performance is analyzed and compared, and the shortcomings in this research are pointed out. The research on the prediction of settlement and deformation of ancient building foundation based on neural networks is very popular. However, there are few

studies linking the depth belief method with it. In this study, the depth belief method is creatively introduced into the conventional GANN. A composite system is established based on the stress analysis of ancient building foundation. The practical significance of this study lies in monitoring and predicting the Settlement and Deformation of Accident Building Foundations (SDABF) and implementing protective measures for buildings. The article aims to inherit history and culture, thereby enriching the entertainment life of residents.

2 Related works

International research is widely distributed in the SDABF prediction. Huan et al. conducted research on various factors that affected the safety status of accident building to improve the accuracy of accident building safety assessment. They proposed a safety assessment model based on the structural entropy weighted matter element extension model. Meanwhile, the weights of each indicator were calculated by taking into account the influence of subjective and objective weights. The museum was used as a research case. The evaluation results were consistent with the actual damage investigation results and the actual situation of the building [5]. An and Sun comprehensively investigated the type of foundations of the adjacent buildings and explored the foundation pit support scheme to ensure the normal use of buildings. The finite difference method was used to analyze building foundation settlement. Reinforced concrete retaining piles were used to excavate and reinforce the foundation pit layer by layer. Their research provided a method for observing the foundation settlement of buildings, providing a good reference for safety assessment and evaluation of similar risk projects [6]. Ye et al. considered that shield tunneling construction would disturb the surrounding soil and affect the safety of nearby buildings. They analyzed the deformation monitoring of arbitrary building structures. A structural deformation monitoring method based on computer vision was developed to perform on-site monitoring of deformation under the influence of shield tunneling. Background correction was used to reduce the error caused by camera position changes. These experiments confirmed that their proposed computer vision method provided an effective method for structural safety assessment [7].

There is an increase in peripheral data during the construction of accidents, relying solely on neural networks for data extraction is insufficient. GANN gradually enters the vision of many scholars. Bozdağ believed that the steep slope of the slope was susceptible to rockfall events. Therefore, experimental investigations and numerical analysis were conducted. The danger of the slope was evaluated. Two-dimensional rockfall analysis was used to determine the jumping distance between detached and suspended blocks. These experiments confirmed that its research results provided preliminary data for describing risk management strategies and made scientific contributions to studying the hazards and risks caused by rockfall phenomena [8]. Borisov et al. described the study of urban construction from the 5th to 8th centuries. They used methods from soil science and archaeological botany. Soil profiles are made at different distances from the settlement. These experiments confirmed the potential risk of foundation settlement and deformation in ancient medieval sites. Burnt grains were used to store in the lower layer of the soil to solve this problem. These experiments confirmed the effectiveness of their method [9]. Di et al. analyzed the settlement of subway lines on soft soil foundations. The combination of different characteristic positions in subway lines was studied. The difference between a track slab and a bridge pier was analyzed. These experiments confirmed that about 85% of the station settlement was smaller than the settlement of adjacent shield tunnels. About 73% of the settlement at the tunnel connection channel was greater than the settlement on both tunnel sides. The stiffness conversion between different structures should be considered when designing subway structures on soft soil foundations [10]. A summary of the relevant works is shown in Table 1.

Table 1: Summary of related works

Author	Time	Main point
Huan et al. [5]	2020	A safety evaluation model of ancient wooden buildings based on the extension model of structural entropy weight is proposed. The influence of subjective and objective weights is considered comprehensively.
An and Sun [6]	2020	The foundation settlement and residual deformation of nearby buildings during subway station construction are analyzed by using finite difference method and deformation observation method.
Ye et al. [7]	2021	The three-dimensional deformation of ancient pagoda under the influence of shield tunnel excavation is monitored by computer vision method.
Bozdağ [8]	2022	The jump distance between the separated block and the suspended block is determined by two-dimensional rock fall analysis.
Borisov et al. [9]	2022	Soil profiles are made at different distances from the settlement.
Di et al. [10]	2020	The measured differential settlement of subway lines is analyzed. The settlement of about 85% stations is less than that of adjacent shield tunnels.

The settlement of about 73% tunnel connecting channels is greater than that on both sides of the tunnels.

To sum up, most of the previous research work focused on a single project example. The established prediction models have insufficient generalization ability. However, these models do not consider the timeliness of the bearing capacity of ancient building foundations under long-term load. That is, these models do not consider the influence of time factors. Neural networks have a strong nonlinear mapping ability. Big data and neural networks are used to analyze the regular trend of the bearing capacity and settlement of pile foundation under long-term load. This paper aims at predicting the bearing capacity and settlement of pile foundation under long-term load. The mathematical model for effectively predicting the bearing capacity and settlement timeliness of ancient building foundation will play a boosting role in the development of the safety evaluation of ancient buildings.

3 The application of GANN in SDABF monitoring and prediction

GANN combines grey system theory with Artificial Neural Network (ANN) and performs superior in prediction performance [11]. GANN improves the traditional grey prediction model and improves the stability of the prediction model by introducing nonlinear fitting ability. This study applies the improved GANN to SDABF monitoring and prediction to avoid problems such as building tilting and cracks.

3.1 Construction of ANN based on DB

The grey prediction model is a prediction method based on a small amount of data, which is suitable for situations such as small data volume and lack of complete information [12]. The grey prediction model describes and predicts the development trend of the system by establishing grey differential formulas. The grey prediction model has certain limitations when dealing with nonlinear and complex systems. GANN introduces ANN into the grey prediction model to fully utilize its nonlinear fitting ability to improve the prediction accuracy of the model. When introduced, the variables in these two models have the relationship in Eq. (1).

$$x_1 = \frac{x - x_0}{x_2 - x_0} \tag{1}$$

In Eq. (1), the random data after ANN enters GANN is denoted as x_1. The minimum and maximum values are represented by x_0, x_2, respectively. x represents the raw data in ANN, which uses the inputting data as the inputting layer of neural network. The predicted results are obtained by calculating and adjusting the hidden layer and outputting layer [13-14]. During the training, GANN continuously adjusts the weights and thresholds of the network through backpropagation to minimize prediction errors. In this process, the weight and threshold calculation of the network follow Eq. (2).

$$\begin{cases} We = (m * R) / A + \beta * (1 - m) \\ Tv = u * \sum_{i=1}^{n} (m * I_i + A * q_i) \end{cases} \tag{2}$$

In Eq. (2), the data step size is denoted as u. m, A represent the environmental errors of data features. The value range of data is represented by n. The number of network layers is denoted as R. β represents the current dimension of the data. I_i and q_i are the resistance to data at different times. The improved GANN has been widely applied in various fields of prediction, especially in the disaster prediction. It can effectively handle nonlinear and time-varying data, which has high predictive stability. However, GANN requires appropriate parameter selection in Eq. (3).

$$\begin{cases} m * Rc - \alpha_1 * Ri \geq 0.9 * Rg \\ Ri_{\min} \geq \alpha_2 * Rt \end{cases} \tag{3}$$

In Eq. (3), Rc represents the compressive strength of the data in GANN. The structural rigidity of network is represented by Ri and is influenced by parameter α_1. The experimental errors caused by gravity and ambient temperature are recorded as Rg and Rt. α_2 is a constant that takes a value within $(1, 2]$ and is related to the minimum Ri [15]. Due to the incomplete and insufficient characteristics of the data processed in this study, SGANN is established in Fig. 1.

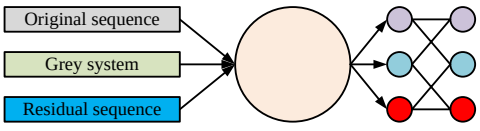

Figure 1: Flow chart of SGANN

From Fig. 1, SGANN combines the grey prediction model in grey system theory with ANN. The grey prediction model serves as the inputting layer. ANN serves as the outputting layer. The study concatenates the two to improve the accuracy and stability of prediction. A grey prediction model is used to preprocess the inputting data to obtain a prediction sequence. Then, the predicted sequence is used as input for further prediction and adjustment through ANN. This model can fully handle

incomplete and uncertain data. Eq. (4) is the variable used when processing data.

$$s = Mo*\left[\sum_{i=1}^{p}\left(\frac{Ex*(\delta_i*\alpha_1)}{\chi*s_i}-\delta_{i-1}*(\alpha_1-1)\right)\right] \quad (4)$$

In Eq. (4), the expansion modulus in SGANN is denoted as Ex, and its expansion fraction is represented by δ_i. Mo represents the original modulus in the model, and its compression factor is denoted as χ. The total number of layers of SGANN is recorded as s. s_i represents the i-th layer within it. In data processing, this study takes into account data collection, transmission, and storage processes to avoid data corruption and ensure data integrity and accuracy. DB and SGANN are integrated in Fig. 2.

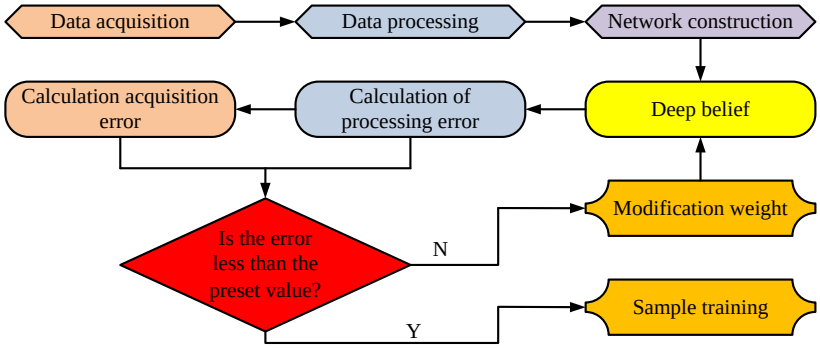

Figure 2: Fusion of depth belief and SGANN

Fig. 2 introduces DB-SGANN. According to Fig. 2, the basic idea of this model is to gradually learn the feature representation of the data from the bottom to the top through layer-by-layer training. Each layer learns some features of the data and passes them on as input to the previous layer. DB-SGANN can extract higher-level features by this layer and training. This model can be applied to data dimensionality reduction. After training, it will learn more abstract feature representations from the original data. In this process, Eq. (5) represents the data conversion before and after dimensionality reduction.

$$\frac{\partial^2(Di)}{\partial(Rd)^2}=\frac{c*\partial^2(E)}{\partial(\rho)^2} \quad (5)$$

In Eq. (5), Di and Rd represent the data before and after dimensionality reduction, respectively. The data density is recorded as ρ. E represents the elasticity between data. c is an internal parameter involved in data collection, which is related to machine performance. This method can reduce the redundancy of data while preserving the main information of the data. Data are analyzed through dimensionality reduction to improve modeling efficiency. In dimensionality reduction, the information preservation of data is balanced against the data information loss in Eq. (6).

$$Se = m*E + f*(E-Ei) \quad (6)$$

In Eq. (6), the retained data is denoted as Se. Ei represents the composite modulus of the compressed data. The weighted environmental resistance in a stationary state is represented by f, which is related to data management methods [16]. The increasing coefficient method is used in Fig. 3. This method achieves data processing by increasing the coefficients of feature vectors. It is suitable for linear data and has high requirements for data distribution and the relationship between features, which meets the requirements of this study.

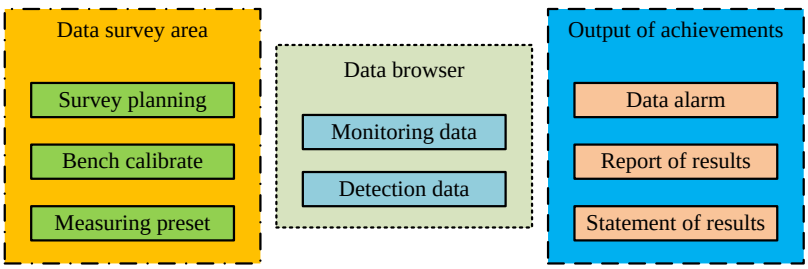

Figure 3: Flow chart of increasing coefficient method

From Fig. 3, the covariance matrix of the original data is first calculated. The eigenvalues are decomposed through the matrix to obtain the eigenvalues and corresponding eigenvectors. The eigenvalues represent the data variance in the corresponding eigenvector direction. The corresponding eigenvectors represent the data distribution in different directions. Based on the set dimensionality reduction goal, retained feature vectors are selected to describe changes in the data. Finally, the retained feature vectors are multiplied with the original data to obtain the managed data. This method can preserve the main information in the original data. Eq. (7) represents the comparison of information intensity between them.

$$Me_1 = \sum_{i=1}^{n} \frac{\Delta Me_i}{Dp_i} * H_i \tag{7}$$

In Eq. (7), the information intensities of the data before and after management are denoted as Me_i, Me_1. The eigenvalues of the covariance matrix are represented by Dp_i . H_i represents the variance of the corresponding feature vector. Through this method, foundation settlement data are input. Potential features in the data are learned using the model. These features can help study the behavior of monitoring and predicting foundation settlement, thus taking corresponding measures for treatment and repair.

In the pre-training stage: first, the state of the hidden node of the first layer network and the state value of the visible node are updated. According to the state value of the visible node, the state of the hidden node is updated again. Then, the offset of the threshold values of visible nodes and hidden nodes is dynamically updated. The state of the hidden node of the first layer network is used as the initial input of the second layer network until the pre-training of the second layer network is completed until the network is trained layer by layer. The matrix vectors of the network weight and threshold are established. The network weight and threshold are updated. The second batch data are input to complete the next round of training until all the data processing is complete.

Prediction and analysis stage: the predicted value is output by softmax function. The data are de-normalized to evaluate the network prediction.

3.2 DB-SGANN and SDABF monitoring and prediction models

Due to the long history of ancient buildings, the bearing capacity of the foundation will be affected, leading to settlement. SDABF is caused by various factors, including the physical properties of the foundation soil and changes in groundwater level. These factors may lead to deformation, thereby affecting the structural safety of the accident building [17-18]. This study draws the arbitrary building foundation map in Fig. 4 and analyzes the properties of the foundation soil to conduct a detailed evaluation of it.

(a) Exterior view of ancient buildings

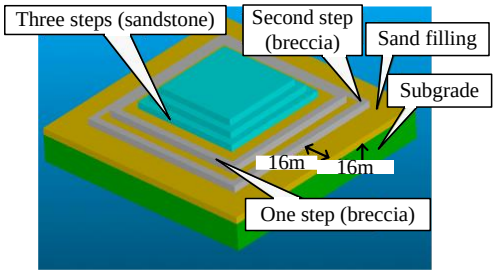

(b) Simplified overall model of the ancient building

Figure 4: Topology diagram of ancient building foundation structure

Fig. 4 (a) is the actual exterior map of the ancient building. According to the actual size of the actual survey data of the ancient building, the main body of the model is basically built according to the real size of the temple structure. To facilitate the simulation and calculation, the central tower, four corner towers of the three-storey platform, four corner towers of the second-storey platform, and two promenade buildings of the first-storey platform are converted into equivalent pressure loads according to their volumes and applied on the surface of the platform. The foundation depth of the model is 16 meters below the surface. The first step is 16 meters in the plane range. This calculation unit adopts the kN and m system. The simplified model is shown in Fig. 4 (b). In Fig. 4 (b), the foundation soil is silty soil sand. The upper layer of foundation soil is filled sand, that is, fine sand. The first and second floors are breccia. The three steps are sandstone. These structures are distributed in the soil. The soil properties have a significant impact on the settlement performance of the foundation. The study establishes the relationship between the various properties of soil and the settlement of the foundation SP in Eq. (8).

$$St = \frac{So_c * \left(So_s + 2h * \tan\left(So_m\right)\right)}{\left(So_t + 2h * \tan\left(So_t\right)\right) * \left(So_p + 2h * \tan\left(So_p\right)\right)} \quad (8)$$

In Eq. (8), the arbitrary building foundation SP is represented by St. So_c represents the compressive performance of the foundation soil. The strength of soil resistance to external forces is recorded as So_s. These two attributes are the inherent properties of soil, and their external factors include water content, saturation, and viscosity, represented by So_m, So_t, So_p, respectively. h represents the depth of excavation, which can affect the stress of the underlying layer of the building foundation. Eq. (9) is the connection between them.

$$Fs = \frac{2 * \left(Ub + Co\right) * h * Ob}{Ub * Co} \quad (9)$$

In Eq. (9), Ub and Co represent the stresses on the upper layer and reinforcement zone, respectively. The total friction force possessed by nearby soil is recorded as Ob, which directly affects the stability of the building. In ancient buildings, the walls supporting the building typically use edge stakes, which are embedded into the building foundation to provide additional durability. In these ancient buildings, edge stakes play an important role, enabling the building to withstand thousands of years without collapsing. Therefore, an architectural diagram of ancient building side piles is drawn based on the internal structure of the building in Fig. 5.

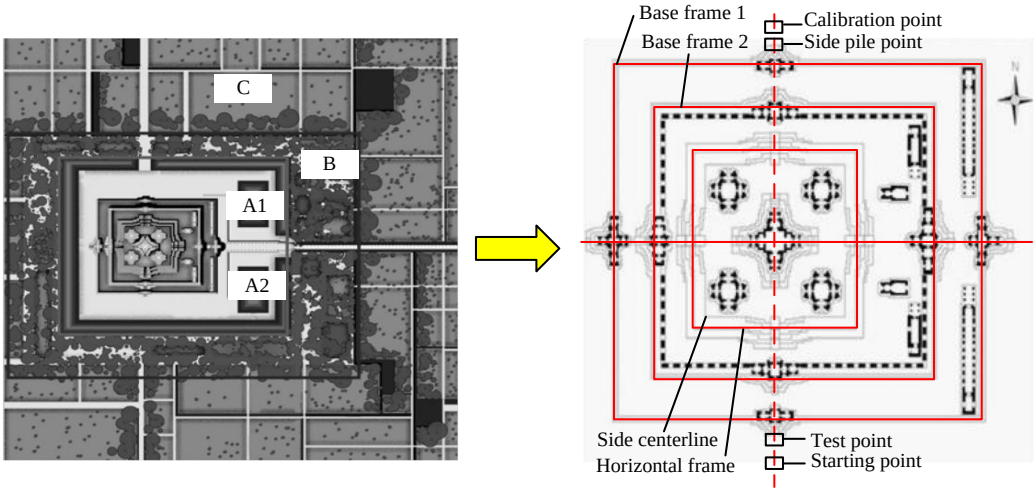

Figure 5: Structural diagram of ancient buildings with side piles

Fig. 5 shows the hierarchical analysis diagram of the edge pile of the accident building. The study first establishes test and calibration points for edge piles in buildings and divides them into basic and horizontal boxes. Then, the starting point and edge pile point are maintained at the lower end of edge pile, both of which are closely related to the settlement of the building. A study is conducted to fuse DB-SGANN with it to generate SPDB-SGANN to analyze its SP capability, with Eq. (10) as the fusion method.

$$Ve_1 = Fs * \frac{\left\| \phi - \varphi_i \right\|^2}{2 * Ve_0} \quad (10)$$

In Eq. (10), the input vector of the fusion model is denoted as Ve_0. The output vector at the SGANN end is represented by Ve_1. The vector of the center points of both is denoted as ϕ. φ_i represents the norm of the vector. At this point, the method can vectorize the obtained data, which has a significant advantage in avoiding redundant data. However, there are differences between the foundation structure of ancient buildings and modern architectures, mainly reflected in the lack of protective structures. Therefore, the ancient buildings are susceptible to external factors such as the hydrological environment in Eq. (11).

$$Wa_s = \sum_{i=1}^{n} Wa_i * T\left(x\right) \quad (11)$$

In Eq. (11), Wa_s is the output value of SPDB-SGANN considering the impact of water environment. The water pressure at each node of the edge pile is represented by Wa_i. n represents the total nodes. The unit influence in this model is represented by $T\left(x\right)$, which is related to the number of perception units in Eq. (12).

$$T\left(x\right) = 0.5 * \sum_{i=1}^{I} \left(t_i - ff_i\right) \quad (12)$$

In Eq. (12), t_i represents the computational layer of neural network. ff_i is the original SDABF data. This method can be used to obtain SDABF prediction model in Fig. 6.

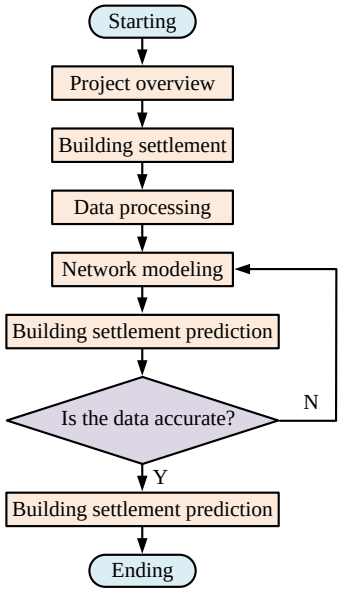

Figure 6: Structure diagram of SDABF prediction

Fig. 6 is an introduction to the SPDB-SGANN prediction of SDABF. From Fig. 6, the study first inputs the geological data of ancient buildings. The factors of foundation settlement are determined according to the data. Then, the mechanical parameters of the soil are tested to calculate the foundation settlement. The settlement of foundation under different load conditions is analyzed based on the soil mechanical parameters and geological data. The parameters for predicting the settlement of ancient building foundation are output. Finally, the weight factors of the model are adjusted based on the proposed model in Eq. (13).

$$Fa_{\eta} = Fa_{\eta-1} + T(x) \tag{13}$$

In Eq. (13), the weight of the model is related to the influence of the model units. Random weight is represented by Fa_{η}. $Fa_{\eta-1}$ represents its nearest neighbor. The feature attention of SPDB-SGANN is optimized through this step, thereby improving the settlement prediction performance of the model. In the actual excavation of foundation, the study calculates the error of geological data in Eq. (14).

$$\begin{cases} Merror = \dfrac{\sum_t \left| \left(Yp_t - Yr\right)_t / Yr_t \right|}{N} \\ Rmse = \left(\dfrac{\sum_t \left(Yp_t - Yr\right)_t^2}{N} \right)^{0.5} \end{cases} \tag{14}$$

In Eq. (14), $Merror$ represents the average error. $Rmse$ represents the root mean square error. Yp, Yr represent the eigenvalues and mean values in the data, and the total number is represented by N. The small Yp, Yr indicate that the predicted and true values have a small difference, indicating good model performance. The adjustment factor of calibration targets is introduced to obtain the minimum value of both in Eq. (15) to evaluate the performance of models between different datasets.

$$\Delta Ad = \mu * \left\| Merror + Rmse \right\|_2^2 * \theta_j \tag{15}$$

In Eq. (15), the adjustment factor of the target is denoted as μ. The total errors before and after adjustment are $\theta_j, \Delta Ad$. This method has good interpretability and intuitiveness in predicting SDABF, which has low sensitivity to outliers.

In this paper, the pre-processed data are input into the network model in the input layer. Feature extraction is carried out in the convolution layer and pooling layer. The extracted features are input into the mean pooling layer for average extraction of all information after the feature extraction of the last layer of pooling layer is completed. Finally, these features are input into the Softmax classifier for data target decision. The extraction operation of feature $y^{l(i,j)}$ is shown in Eq. (16).

$$y^{l(i,j)} = \sum_{j\hat{}=0}^{W-1} K_i^{l(j\hat{})} x^{l(j+j\hat{})} \tag{16}$$

In Eq. (16), $K_i^{l(j\hat{})}$ represents the l weight of the i convolution kernel in the $j\hat{}$ layer. $x^{l(j+j\hat{})}$ represents the l target region in the j layer. W is the width of the convolution kernel. The input layer is the time-frequency graph of training bearings. The convolution kernel size of the first layer is 5*5. The step size is 2*2. The convolution kernel of the second and third layers is 3*3. The step size of the third layer is 2*2. The size of the pooling region of the three layers is 2*2. It is necessary to fill the eigenvalues to keep the size of the eigenvalues after each convolution and pooling unchanged. That is, adding zeros around the feature map makes the feature map complete.

Next, the SPDB-SGANN algorithm network conducts self-learning to train the neural network model until the error between the theoretical output value and the actual output value reaches the minimum. The network training time is too long due to the excessive number of samples in the training set and the one-time training of so many data sets. Meanwhile, the network parameters (weights and biases) are updated slowly, resulting in poor results. Therefore, 128 groups are randomly selected from all training data each time to update and train network parameters. The convolutional layer in the network model uses Relu activation function. The fully connected layer uses Sigmoid activation function. The learning efficiency of the Adam optimization algorithm is 0.001. The dropout is set to 0.5 to prevent overfitting of the training process data.

4 Application effect of composite model SPDB-SGANN in SDABF monitoring and prediction

This study conducted SDABF monitoring and prediction experiments on the Abfound dataset to analyze the practical application effect of the model. In this dataset, there were a total of 2520 pieces of data on building foundations of different ages, including various terrains such as sand and tundra. Therefore, experiments were conducted on two parameters of existence time and geographical location, respectively, on the included accident building.

4.1 The predictive ability and internal performance of SPDB-SGANN in SDABF

The settlement prediction model was established using MATLAB software. The relevant parameters were set as follows: the maximum number of iterations of the neural network was 10, the maximum number of trainings was 100, the learning rate was 0.01, and the minimum error of the training target was 0.001. The neural network structure was determined as 4-9-1 (4 neurons in the input layer, 9 neurons in the hidden layer, and 1 neuron in the output layer). 36 weights from the input layer to the hidden layer, 9 weights from the hidden layer to the output layer, and 10 thresholds were obtained. The 55 weights and thresholds of the neural network were optimized. The optimal initial weights and thresholds were assigned to the neural network for settlement prediction. The model was used for simulation training. The predicted values of the neural network before and after optimization were compared with the measured values.

Due to the limited data in Abfound, this study evenly divided it into two groups. The incidence building types in each group were basically the same. The equipment selection and parameter settings in the experiment were first conducted before the experiment to carry out the experiment effectively. Then, the internal performance test of SPDB-SGANN was conducted. Meanwhile, experiments were conducted on Random Forest (RF), Artificial Fish Swarm Algorithm (AF), and Generalized Predictive Control (GPC) to validate the superiority of the proposed model in Fig. 7.

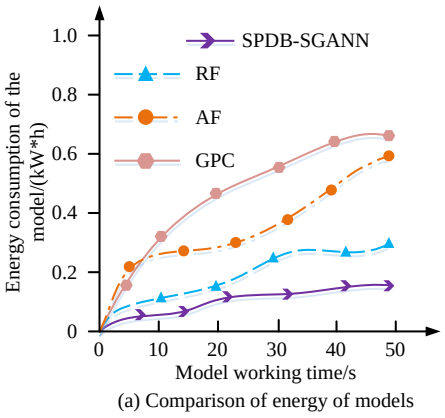

(a) Comparison of energy of models

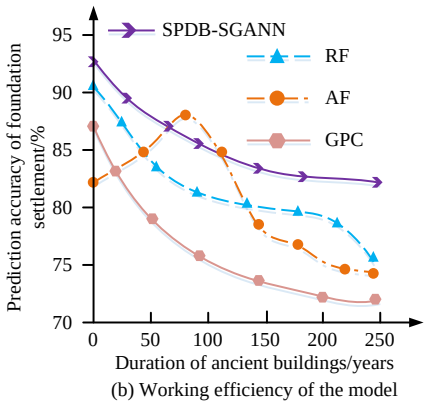

(b) Working efficiency of the model

Figure 7: Comparison diagram of internal performance test of model in foundation deformation of ancient buildings

Fig. 7 shows a comparative experiment on the internal performance of four models in soil deformation. According to Fig. 7(a), as the working hours increased, the energy losses of the four models also increased. The energy consumption of SPDB-SGANN was the lowest, at 0.15 kW*h. The results of RF, AF, and GPC were 0.23, 0.58, and 0.64 kW*h, respectively. This indicated that the composite model proposed had the highest utilization rate for the same accident building. In Fig. 7(b), the duration of the building's existence was inversely proportional to the accuracy of the model's settlement prediction. The accuracy rates of SPDB-SGANN, RF, AF, and GPC for predicting settlement of 250-year buildings were 84.8%, 76.2%, 74.9%, and 72.7%, respectively. The settlement prediction accuracy of its SPDB-SGANN was the highest, indicating that the model had the best performance. Data fluctuation experiments were conducted on these four models to more accurately demonstrate the overall internal performance of the model in Fig. 8.

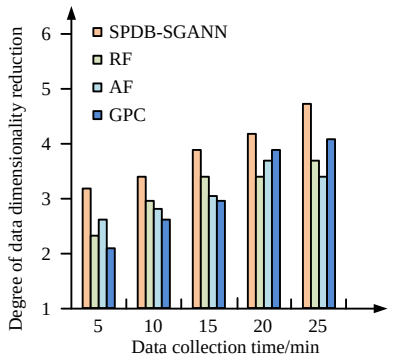

(a) Data dimension reduction experiment

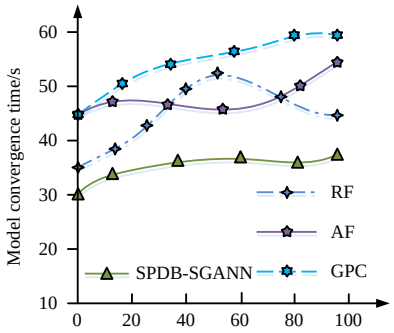

(b) Model convergence experiment

Figure 8: Comparison chart of experimental results of data fluctuation of four models

Fig. 8 shows the comparison of the data dimensionality reduction and convergence experiments of four models. In Fig. 8(a), the data dimensionality reduction of the model continued to improve. For this parameter, if the data were above 3.5, the requirements of the foundation settlement prediction experiment for ambient building were met. The data dimensionality reduction performance of SPDB-SGANN was the best, at 4.6. The experimental data for other three models at this time were 3.6, 3.2, and 3.9, respectively. After the same working time, the data obtained by SPDB-SGANN were the best. This conclusion was also presented in Fig. 8(b). The convergence time of the four models was 34s, 44s, 53s, and 59s, respectively. This indicated that SPDB-SGANN had the shortest working time for ancient buildings with the same radius. However, the above experiments could only demonstrate the superior internal performance of the model. Experimental verification was also required for the practical performance of the model.

Based on predictions and true labels, the samples are divided into four categories: True Positive (TP), True Negative (TN), False Positive (FP) and False Negative (FN). The performance of SPDB-SGANN model was verified by calculating the accuracy rate, accuracy rate, recall rate, and F1 value. From Table 2, the prediction accuracy of the research model for the foundation settlement of ancient buildings reached 96.15%. The accuracy rate was 96.17%, the recall rate was 86.15%, and the F1 value was 96.16%, all of which were higher than the comparison models. In general, the SPDB-SGANN model proposed in this paper had a high performance in the prediction of foundation settlement of ancient buildings.

Table 2: Comparison of prediction accuracy of settlement of ancient buildings by different models

Model	Accuracy (%)	Precision (%)	Recall (%)	F1 value (%)
RF	64.99	65.16	64.99	65.09
AF	82.06	82.27	82.06	82.17
GPC	85.77	85.87	85.76	85.82
SPDB-SGANN	96.15	96.17	96.15	96.16

4.2 Experimental verification of SPDB-SGANN in SDABF monitoring and prediction

Stress and model performance tests on buildings were conducted to verify the practical application efficiency of SPDB-SGANN in SDABF in Fig. 9.

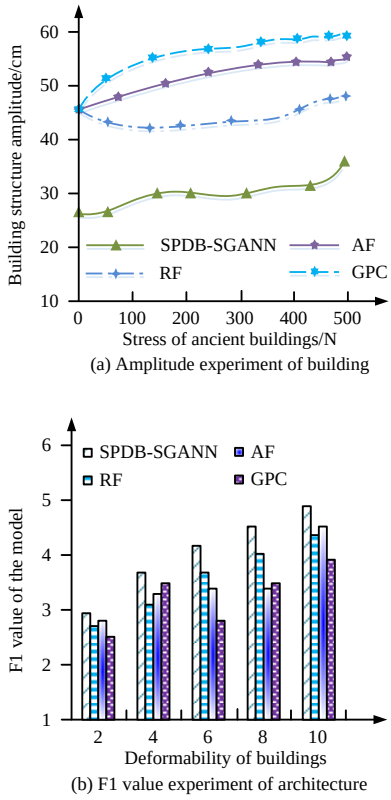

Figure 9: Comparison chart of field test results of four models

Fig. 9 shows the experimental results of building stress and harmonic mean values. SPDB-SGANN exhibited the best architectural amplitude performance at 28 cm, while the other three models were 43 cm, 52 cm, and 55 cm, respectively. This indicated that SPDB-SGANN had the best experimental effect on building performance for ancient buildings under the same stress. This phenomenon could also be verified in Fig. 9(b). The harmonic mean values of four models were 4.7, 4.2, 4.4, and 3.9, respectively. The proposed composite model achieved the best experimental effect in the same settlement of ancient building. Node experiments and foundation settlement experiments were conducted to control the impact of hidden nodes in the model on the experimental results in Fig. 10.

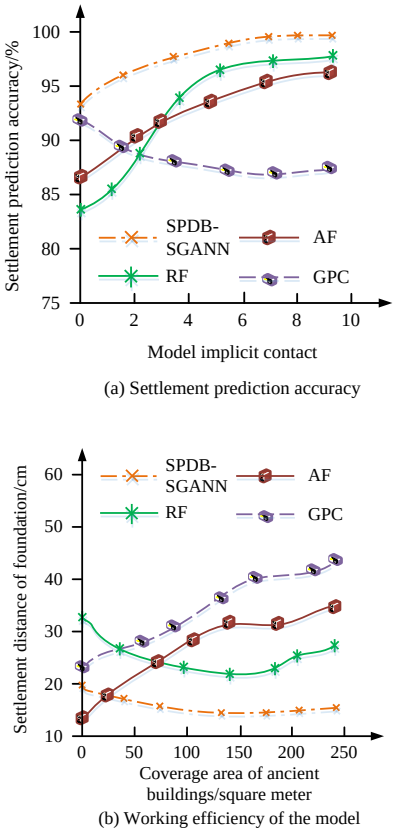

Figure 10: Comparison diagram of hidden node experiment and foundation settlement experiment of four models

Fig. 10 shows the comparison of the hidden nodes and foundation settlement of the four models. In Fig. 10(a), the accuracy of building settlement prediction increased with the increase of nodes. SPB-SGANN achieved the highest SDABF prediction accuracy of 99.2%. The other three models only had prediction accuracy of 96.3%, 94.9%, and 88.7% at this time, respectively. The proposed composite model had higher accuracy for the same hidden nodes. In Fig. 10(b), the settlement distance of the building was positively correlated with the occupied area of building. The SPDB-SGANN building had the highest stability with a settlement distance of 14 cm. The other three models had a settlement distance of 24 cm, 31 cm, and 40 cm, respectively. The proposed composite model could provide the best settlement protection for buildings. However, the results of a single experiment couldn't demonstrate the universality of the model, so the study conducted 30 experiments and drew a linear fitting graph in Fig. 11.

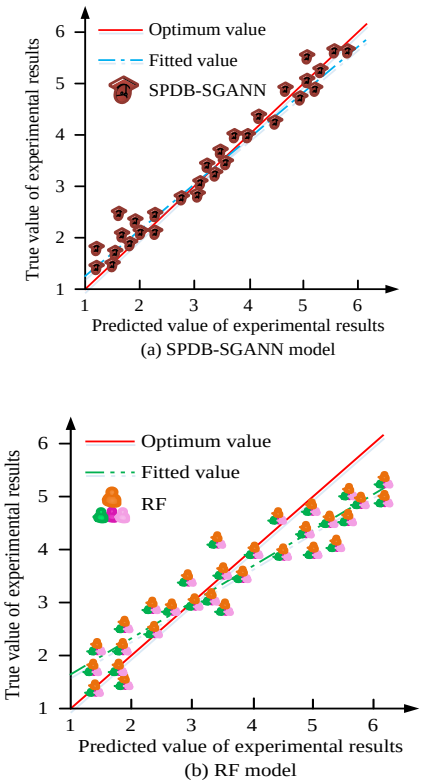

Figure 11: Extensive experiment of SPDB-SGANN model

Fig. 11 shows a comprehensive experimental demonstration of the proposed composite model. In 30 comparative experiments, the test values of SPDB-SGANN were closer to the true values, with a linear fit of 0.9996. The experimental results of RF were relatively distant, with a linear fit of only 0.9764. These experiments had confirmed that SPDB-SGANN could effectively predict and detect SDABF, making it suitable for security protection in ancient buildings.

The actual verification was carried out with an ancient building. The location of observation points is shown in Fig. 12. The ancient building has a square plan and its main structure is composed of five square stone towers arranged on the base of a three-story flat-topped pyramid. The inner and outer walls connect the four gates in the east, west, south and north. The Temple Mountain building is surrounded by a gully. The Shinto Road is built on the east side. Two pools are set symmetrically on both sides of the Shinto Road. The foundation of the ancient building adopts the method of building a high platform. There is a platform on the large platform. There are large stone masonry around the platform.

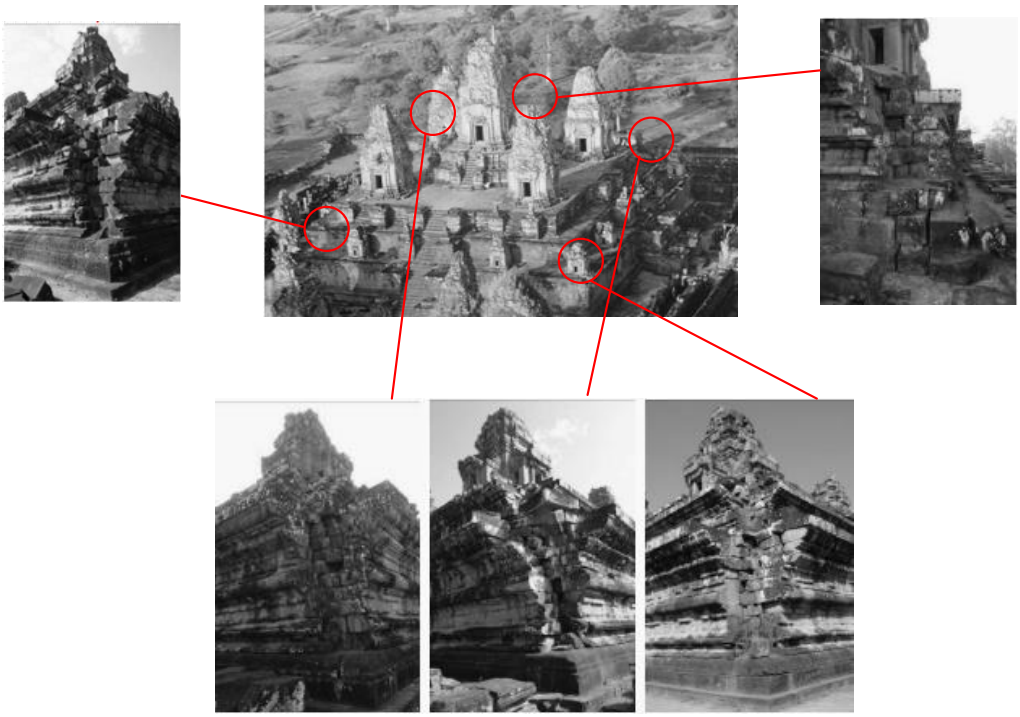

Figure 12: Schematic diagram of location arrangement of observation points

Table 3 shows the comparison of the prediction results of the three prediction models. The error was positive, the predicted value was greater than the measured value, and vice versa was less than the measured value. The general predicted results were all too large. The reason for these errors is that the maximum settlement value of the near shallow foundation of these measured data is the maximum settlement value of the set

measurement point, which is mostly set only on both sides of the building. In actual projects, the location of the building and whether the construction is standardized may have an impact on the location of the maximum settlement point. SPDB-SGANN had the best prediction performance, with the maximum error of 46.45mm and the minimum error of 8.51mm. These results were better than the other two models, providing a preliminary prediction for the settlement of ancient buildings. This model can meet the requirements.

Table 3: Comparison of the prediction results of the test group of the three prediction models

Serial number	Measured settlement value (mm)	SPDB-SGANN		AF		RF	
		Predicted value (mm)	Error (mm)	Predicted value (mm)	Error (mm)	Predicted value (mm)	Error (mm)
1	3.70	38.56	34.86	65.38	61.68	68.08	64.38
2	0.80	13.59	12.79	9.73	8.93	-20.22	-21.02
3	5.60	-.297	-8.51	14.73	9.13	17.76	12.16
4	15.60	62.05	46.45	15.14	-0.46	200.93	185.33
5	15.48	26.94	11.54	-36.13	-51.53	77.33	61.93

The prediction accuracy of 30 experiments was calculated. Fig. 13 shows the T-test statistical results of the proposed composite model (different letters indicate significant differences, $P<0.05$). In 30 experiments, the average accuracy of SPDB-SGANN model reached 98.06%, which was the highest among all models. The difference was significant compared with AF, RF, and GPC ($P>0$).

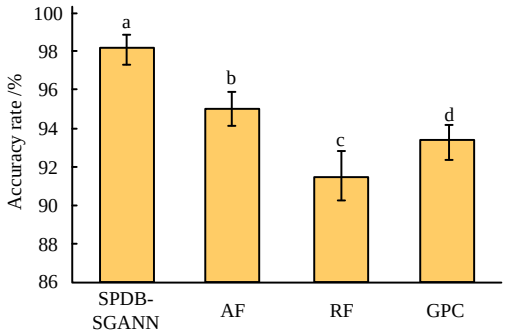

Figure 13: Accuracy significance test results

5 Results and discussion

Du et al. selected the base modulus, Young's modulus, field soil properties and applied load as the input of the model to establish a GP-ANN model to estimate the maximum settlement of the ERP system. The prediction results of the GP-ANN model were compared with those of other neural network models. The prediction effect of the GP-ANN model was superior [19]. The construction form, algorithm flow, performance and defects of the GM-BPNN model were summarized. SPB-SGANN had the best data dimension reduction performance (4.6). At this time, the experimental data of the other three models were 3.6, 3.2, and 3.9, respectively. After the same working hours, SPB-SGANN obtained the best data. Through model comparison and analysis, the GA-GM-BPNN model had good prediction accuracy and prediction precision in short-term deformation prediction, high reliability of deformation extraction, and superior prediction performance.

Wu et al. selected effective pile length, flexural stiffness of piles, applied load, friction angle of sand piles and ratio of pile length to width as the input of ANN based on the static load test data of steel piles with expanded bottom. Then, the ANN prediction model of pile foundation settlement was established. The predicted value of the model was very close to the measured value. The mean square error was relatively not obvious [20]. Zhang et al. combined ANN and heuristic algorithm (equilibrium optimizer EO) to provide an efficient and reliable prediction model for pile foundation settlement calculation [21]. The SPB-SGANN settlement prediction model of ancient buildings was constructed. This model improved the ability of deformation extraction and nonlinear problem processing, accelerated the speed of model convergence, and solved the oscillation prediction of the original model. SPB-SGANN had the highest prediction accuracy of 99.2%. AF\RF\GPC had the prediction accuracy of 96.3%, 94.9%, and 88.7%, respectively. The proposed composite model can provide the best settlement protection for buildings. However, the results of a single experiment do not prove the universality of the model. Therefore, through 30 comparative experiments, the test value of SPB-SGANN was closer to the true value, with a linear fit of 0.9996. The accumulation of errors in the model training process was small, which was suitable for the extraction and mining of long-sequence super-tall deformation sequences.

6 Conclusion

With the modernization of the information industry, ancient buildings' protective measures are gradually developing. DB was introduced into SGANN. A composite model (SPDB-SGANN) was generated to cope with the increasing amount of data. Experiments were conducted on and compared with the experimental results of RF, AF, and GPC to verify the effectiveness and universality of the model. Under the same working hours, the energy losses of four models were 0.15, 0.23, 0.58, and 0.64 kW*h, respectively, indicating that SPDB-SGANN had the highest economic benefits. For the 250-year SDABF prediction, the proposed composite model had an accuracy of 84.8% and performed best among the four models, indicating that the model had the best performance. In the data dimensionality reduction experiment, the results of SPDB-SGANN, RF, AF, and GPC were 4.6, 3.6, 3.2, and 3.9, respectively, indicating that the model could effectively sort out complex data. In ancient buildings with the same radius, the convergence time of SPDB-SGANN was 34 seconds, which was the fastest among four models, indicating that this model had the lowest time cost. For buildings with the same settlement, the harmonic average values of four models were 4.7, 4.2, 4.4, and 3.9, respectively. This indicated that SPDB-SGANN could provide the strongest control over buildings. In experiments with the same hidden nodes, SPDB-SGANN had the highest SDABF prediction accuracy of 99.2%. The other three models had prediction accuracy of 96.3%, 94.9%, and 88.7%, respectively. This indicated that the model could effectively utilize hidden nodes. In 30 extensive experiments, the linear fit of SPDB-SGANN and RF was 0.9996 and 0.9764, respectively. These experiments confirmed that the proposed SPDB-SGANN could accurately detect and predict foundation settlement of ancient buildings. However, this study only focuses on ancient buildings and has no reference significance for modern architecture. This is because the completion year of modern architecture is too short, and the experimental results are not convincing. With the improvement of the experimental setup, studies will gradually be conducted on modern architecture in the future.

7 Funding

The research is supported by Henan Province Science and Technology Research Project: Research on Real Time Monitoring and Early Warning System for Building Heritage Foundation Settlement, Project number: 222102320368; Henan Province Science and Technology Research Project: Research on the Reinforcement and Mechanical Properties of Wood Structure Columns in Historical Buildings, Project number: 232102320170; Real-time Monitoring and Early Warning Research on Tilt of Ancient Buildings in Nanyang City in 2023 Science and Technology Development Plan, Project Number: 23RKX005.

References

[1] S. Maruoka, H. Tabuchi, D. Nagasato, H. Masumoto, T. Chikama, A. Kawai, N. Oishi, T. Maruyama, Y. Kato, T. Hayashi, and C. Katakami, "Deep neural network-based method for detecting obstructive meibomian gland dysfunction with in vivo laser confocal microscopy," Cornea, vol. 39, no. 6, pp. 720-725, 2020. https://doi.org/10.1097/ICO.0000000000002279

[2] S. Admasie, S. Bukhari, T. Gush, R. Haider, and C. Kim, "Intelligent islanding detection of multi-distributed generation using artificial neural network based on intrinsic mode function feature," Journal of Modern Power Systems and Clean Energy, vol. 8, no. 3, pp. 511-520, 2020. https://doi.org/10.35833/MPCE.2019.000255

[3] P. K. Kushwaha, S. P. Maurya, P. Rai, and N. Singh, "Porosity prediction from offshore seismic data of F3 Block, the Netherlands using multi-layer feed-forward neural network," Current Science, vol. 119, no. 10, pp. 1652-1662, 2020. https://doi.org/10.18520/cs/v119/i10/1652-1662

[4] C. Zhang, Y. Zhao, Y. Zhou, X. Zhang, and T. Li, "A real-time abnormal operation pattern detection method for building energy systems based on association rule bases," Building Simulation, vol. 15, no. 1, pp. 69-81, 2022. https://doi.org/10.1007/s12273-021-0791-x

[5] J. Huan, D. Ma, W. Wang, X. Guo, Z. Wang, and L. Wu, "Safety-state evaluation model based on structural entropy weight-matter element extension method for ancient timber architecture," Advances in Structural Engineering, vol. 23, no. 6, pp. 1087-1097, 2020. https://doi.org/10.1177/1369433219886085

[6] J. B. An, and C. F. Sun, "Safety assessment of the impacts of foundation pit construction in metro station on nearby buildings," International Journal of Safety and Security Engineering, vol. 10, no. 3, pp. 423-429, 2020. https://doi.org/10.18280/ijsse.100316

[7] X. Ye, T. Jin, P. Ang, C. Xue, and C. Yun, "Computer vision-based monitoring of the 3-D structural deformation of an ancient structure induced by shield tunneling construction," Structural Control and Health Monitoring, vol. 28, no. 4, pp. e1-23, 2021. https://doi.org/10.1002/stc.2702

[8] A. Bozdağ, "Rockfall hazard assessment in a natural and historical site: The case of ancient Kilistra settlement (Konya), Turkey," Journal of Mountain Science, vol. 19, no. 1, pp. 151-166, 2022. https://doi.org/10.1007/s11629-021-6961-6

[9] A. Borisov, D. Korobov, A. Sergeev, and N. Kashirskaya, "Traces of ancient agriculture in the soil around the archaeological sites (A case study

from Northern Caucasus, Russia)," Quaternary International, vol. 618, pp. 4-13, 2022. https://doi.org/10.1016/j.quaint.2020.12.028

[10] H. Di, S. Zhou, P. Guo, C. He, X. Zhang, and S. Huang, "Observed long-term differential settlement of metro structures built on soft deposits in the Yangtze River Delta region of China," Canadian Geotechnical Journal, vol. 57, no. 6, pp. 840-850, 2020. https://doi.org/10.1139/cgj-2018-0524

[11] J. B. Sun, "Prediction and estimation of book borrowing in the library: Machine learning," Informatica: An International Journal of Computing and Informatics, vol. 45, no. 1, pp. 163-168, 2021. https://doi.org/10.31449/inf.v45i1.3431

[12] Y. Guo, Z. Mustafaoglu, and D. Koundal, "Spam detection using bidirectional transformers and machine learning classifier algorithms," Journal of Computational and Cognitive Engineering, vol. 2, no. 1, pp. 5-9, 2022. https://doi.org/10.47852/bonviewJCCE2202192

[13] V. Andrushko, "Revelations of ancient head shape: Cranial modification in the Cuzco region of Peru, Early Horizon to Inca Imperial Period," American Journal of Physical Anthropology, vol. 175, no. 1, pp. 95-105, 2021. https://doi.org/10.1002/ajpa.24201

[14] J. Lobo, L. Bettencourt, M. Smith, and S. Ortman, "Settlement scaling theory: Bridging the study of ancient and contemporary urban systems," Urban Studies, vol. 57, no. 4, pp. 731-747, 2020. https://doi.org/10.1177/0042098019873796

[15] M. Zhou, X. Su, J. Lei, and S. Fang, "Foundation reinforcement and deviation rectification of the leaning pagoda of Dinglin temple, China," Proceedings of the Institution of Civil Engineers-Geotechnical Engineering, vol. 173, no. 6, pp. 473-484, 2020. https://doi.org/10.1680/jgeen.19.00028

[16] R. Ranjan, and A. K. Daniel, "CoBiAt: A sentiment classification model using hybrid ConvNet-Dual-LSTM with attention techniques," Informatica: An International Journal of Computing and Informatics, vol. 47, no. 4, pp. 523-536, 2023. https://doi.org/10.31449/inf.v47i4.3911

[17] A. Bahuguna, and C. Thakar, "Archaeological exploration of defence structures & fortress city based on ancient folklore of Mount Abu, Rajasthan, India," International Journal of Management and Humanities, vol. 4, no. 8, pp. 99-103, 2020. https://doi.org/10.35940/ijmh.H0832.044820

[18] C. Guo, "The evaluation model of reconstruction effect of ancient villages under the influence of epidemic situation based on big data," Journal of Intelligent and Fuzzy Systems, vol. 39, no. 6, pp. 8813-8821, 2020. https://doi.org/10.3233/JIFS-189278

[19] X. Du, X. Ran, and W. Di, "Research on spatial perception and inheritance of traffic settlement: a case study of Yuliang ancient village in Huizhou," Journal of Landscape Research, vol. 14, no. 2, pp. 123-129, 2022.

[20] Z. Wu, X. Fang, D. Jia, and G. Zhao, "Reconstruction of cropland cover using historical literature and settlement relics in farming areas of Shangjing Dao during the Liao dynasty, China, around 1100 AD," The Holocene, vol. 30, no. 2, pp. 1516-1527, 2020. https://doi.org/10.1177/0959683620941293

[21] D. Zhang, A. Polamarasetty, M. O. Shahid, B. Krishnaswamy, and C. Ma, "Passive mechanical vibration processor for wireless vibration sensing," Applied Physics, 2023. https://doi.org/10.48550/arXiv.2305.10687